Original Research

Mevalonate depletion mediates the suppressive impact of geranylgeraniol on murine B16 melanoma cells

Rajasekhar Katuru[1], Nicolle V Fernandes[1], Manal Elfakhani[1], Dibyendu Dutta[2], Nathaniel Mills[2], DiAnna L Hynds[2], Clay King[1] and Huanbiao Mo[1]

[1]Department of Nutrition and Food Sciences; [2]Department of Biology, Texas Woman's University, P.O. Box 425888, Denton, TX 76204, USA

Corresponding author: Huanbiao Mo. Email: hmo@mail.twu.edu

Abstract

The diterpene geranylgeraniol (all *trans*-3,7,11,15-tetramethyl-2,6,10,14-hexadecatetraen-1-ol) suppresses the growth of human liver, lung, ovary, pancreas, colon, stomach and blood tumors with undefined mechanisms. We evaluated the growth-suppressive activity of geranylgeraniol in murine B16 melanoma cells. Geranylgeraniol induced dose-dependent suppression of B16 cell growth ($IC_{50} = 55 \pm 13$ μmol/L) following a 48-h incubation in 96-well plates. Cell cycle arrest at the G1 phase, manifested by a geranylgeraniol-induced increase in the G1/S ratio and decreased expression of cyclin D1 and cyclin-dependent kinase 4, apoptosis detected by Guava Nexin™ assay and fluorescence microscopy following acridine orange and ethidium bromide dual staining, and cell differentiation shown by increased alkaline phosphatase activity, contributed to the growth suppression. Murine 3T3-L1 fibroblasts were 10-fold more resistant than B16 cells to geranylgeraniol-mediated growth suppression. Geranylgeraniol at near IC_{50} concentration (60 μmol/L) suppressed the mRNA level of 3-hydroxy-3-methylglutaryl coenzyme A (HMG-CoA) reductase by 50%. The impact of geranylgeraniol on B16 cell growth, cell cycle arrest and apoptosis were attenuated by supplemental mevalonate, the product of HMG-CoA reductase that is essential for cell growth. Geranylgeraniol and *d*-δ-tocotrienol, a down-regulator of HMG-CoA reductase, additively suppressed the growth of B16 cells. These results support our hypothesis that mevalonate depletion mediates the tumor-specific growth-suppressive impact of geranylgeraniol. Geranylgeraniol may have potential in cancer chemoprevention and/or therapy.

Keywords: geranylgeraniol, B16 melanoma, HMG-CoA reductase, mevalonate, cell cycle, apoptosis, differentiation

Experimental Biology and Medicine 2011; **236**: 604–613. DOI: 10.1258/ebm.2011.010379

Introduction

The mevalonate-derived intermediates, farnesyl pyrophosphate and geranylgeranyl pyrophosphate, are covalently attached to the carboxy-terminal cysteine residue of the nuclear lamins[1] and members of the small G proteins.[2] This post-translational modification is essential to the membrane attachment and biological functions of these proteins that are vital to cell survival and growth.

3-Hydroxy-3-methylglutaryl coenzyme A (HMG-CoA) reductase, the rate-limiting activity in mevalonate synthesis,[3] is differentially regulated in sterologenic and tumor tissues.[4] In sterologenic tissues, HMG-CoA reductase is under a multivalent regulation consisting of sterol-mediated transcriptional feedback regulation and non-sterol-mediated post-transcriptional regulation. Tumor reductase activity, to the contrary, is resistant to the sterol-mediated transcriptional regulation and consequently elevated. Nevertheless, tumor reductase remains responsive to the isoprenoid-mediated downregulation.

The essential role of mevalonate in growth and the uniquely dysregulated tumor HMG-CoA reductase render the tumor reductase a viable target for intervention. The statins, competitive inhibitors of HMG-CoA reductase,[3] and the isoprenoids, down-regulators of reductase,[5] suppress the growth of melanoma cells. Geranylgeraniol (all *trans*-3,7,11,15-tetramethyl-2,6,10,14-hexadecatetraen-1-ol), a diterpene found in linseed oil,[6] *Cedrela toona* wood oil[7] and sucupira branca fruit oil,[8] suppresses HMG-CoA reductase activity in human fibroblasts[9,10] and human A549 lung adenocarcinoma cells.[11] Geranylgeraniol also suppresses the proliferation of tumor cells derived from human blood,[12–15] lung,[11,16,17] colon,[13,14] liver,[14,18] ovary,[14,19] pancreas[14,20] and stomach.[14] Nevertheless, the role of mevalonate in geranylgeraniol-mediated growth inhibition has not been delineated.

We hypothesize that mevalonate depletion mediates the growth-suppressive impact of geranylgeraniol in tumors. In the present study we tested this hypothesis in murine B16 melanoma cells. Geranylgeraniol-induced concentration-dependent suppression of the B16 cell growth was accompanied by cell cycle arrest at the G1 phase, initiation of apoptosis and increased alkaline phosphatase (ALP) activity suggesting cell differentiation. Supplemental mevalonolactone attenuated the impact of geranylgeraniol on cell growth, cell cycle arrest and apoptosis. Blends of geranylgeraniol and *d*-δ-tocotrienol, a down-regulator of HMG-CoA reductase activity, synergistically suppressed the growth of B16 cells.

Materials and methods

Chemicals

Lovastatin and *d*-δ-tocotrienol were gifts from Merck Research Laboratories (Rahway, NJ, USA) and American River Nutrition, Inc (Hadley, MA, USA), respectively. Geranylgeraniol was purchased from Sigma-Aldrich (St Louis, MO, USA).

Cell growth assay

Murine B16 melanoma cell growth was measured by using CellTiter 96® Aqueous One Solution (Promega, Madison, WI, USA) as previously described.[21] Briefly, B16 melanoma cells, purchased from the American Type Culture Collection (ATCC, Manassas, VA, USA) and cultured in RPMI 1640 medium (Sigma-Aldrich) supplemented with 10% fetal bovine serum (Hyclone Lab Inc, Logan, UT, USA) and 1% penicillin–streptomycin (MP biomedicals, Solon, OH, USA) at 37°C in a humidified atmosphere of 5% CO_2 were seeded at 1000 cells/0.1 mL medium/well in 96-well tissue culture plates (Fisher Scientific Company LLC, Houston, TX, USA). At 24 h, the medium was decanted from each well and replaced with 0.1 mL fresh medium containing geranylgeraniol that was pre-dissolved in ethyl alcohol. All cultures contained 1 mL/L of ethyl alcohol. Cells were further incubated for an additional 48 h. The 72-h cell populations following a quick rinse with 0.1 mL Hank's Balanced Salt Solution were determined by adding 20 μL of CellTiter 96® Aqueous One Solution to each well; plates were held in the dark at 37°C for two hours and then read at 490 nm with a SPECTRAmax® 190 multi-plate reader with SOFTmax® PRO version 3.0 (Molecular Devices, Sunnyvale, CA, USA). Absorbances from wells containing cell-free medium were used as baselines and were deducted from absorbances of other cell-containing wells. The IC_{50} value is the concentration of geranylgeraniol required to suppress the net increase in cell number by 50%.

Murine 3T3-L1 embryo fibroblasts (ATCC) were grown in Dulbecco's modified Eagle's medium with 4 mmol/L L-glutamine adjusted by ATCC to contain 1.5 g/L sodium bicarbonate and 4.5 g/L glucose, supplemented with 10% bovine calf serum and 1% penicillin/streptomycin (Invitrogen, Carlsbad, CA, USA). Cultures, seeded in 0.1 mL medium with 2×10^3 cells/well in a 96-well plate, were incubated for 24 h at 37°C in a humidified atmosphere of 5% CO_2. At 24 h, the medium was decanted from each well and replaced with 0.1 mL fresh medium containing geranylgeraniol. Incubation continued for an additional 48 h. Cell populations of all wells were determined using the CellTiter 96® Aqueous One Solution.

Microscopy

Photomicrographs of representative fields of monolayers of B16 cells in the cell growth assay were made with a Nikon Eclipse TS 100 microscope (Nikon Corporation, Tokyo, Japan) equipped with a Nikon Coolpix 995 digital camera (Nikon Corporation).

Cell cycle distribution

B16 cells were seeded in 25-cm^2 flasks (Becton Dickinson Labware, Franklin Lakes, NJ, USA) at 1×10^6 cells/flask with 5 mL medium/flask and incubated for 24 h. The medium was then decanted and cultures were replenished with medium containing geranylgeraniol that had been dissolved in ethyl alcohol. Following additional 12- and 24-h incubations, adherent cells were harvested by trypsinization and pelleted by low speed centrifugation. Cell pellets were fixed in 1 mL 70% ethanol at −20°C overnight and washed in 1 mL phosphate-buffered saline (PBS). Cells (5×10^5) were re-suspended in 500 μL PBS containing 0.5 mg RNase A (Sigma-Aldrich) and incubated at 37°C for 30 min. Following gentle mixing, a 100 μL aliquot of propidium iodide (Sigma-Aldrich; 1 g/L in PBS containing 0.1% Triton X-100) was added. The cells were incubated in the dark at room temperature for 15 min and then held at 4°C in the dark for flow cytometric analysis.[22] Aliquots of 1×10^4 cells were analyzed for DNA content using a BD FACSCaliber™ Flow Cytometer (BD Biosciences, San Jose, CA, USA). The distribution of cells in the G1, S and G2/M phases of the cell cycle was determined using MultiCycle AV software (Phoenix Flow Systems, San Diego, CA, USA).

Annexin V assay for apoptosis

B16 cells were seeded in 25-cm^2 flasks (Becton Dickinson Labware) at 1×10^6 cells/flask with 5 mL medium/flask and incubated for 24 h. Medium was then decanted and cultures were replenished with medium containing geranylgeraniol. Following additional 12- and 24-h incubations, adherent cells were harvested by trypsinization and pelleted by refrigerated centrifugation at 300*g* for 10 min. Re-suspended cells in 150 μL medium containing 2×10^4 cells were mixed with 50 μL of the Guava Nexin™ reagent containing Annexin V-PE and Nexin 7-amino-actinomycin D (7-AAD), loaded onto the 96-well plate and incubated at room temperature in the dark for 20 min. Samples containing 5×10^3 cells were analyzed by using a Guava EasyCyte flow cytometer (Guava Technologies, Inc, Hayward, CA, USA) with the Guava ExpressPlus program.[22,23] Annexin V is a phospholipid-binding protein that has high affinity for phosphatidylserine translocated from the internal surface to the outer surface of

cell membrane at the early stage of apoptosis. 7-AAD selectively permeates late stage apoptotic and dead cells. Therefore cells that are viable (Annexin V− and 7-AAD−), early apoptotic (Annexin V+ and 7-AAD−), late apoptotic (Annexin V+ and 7-AAD+) and dead cells with nuclear debris (Annexin V− and 7-AAD+) can be separated and percentages of these cell populations quantified.

Acridine orange and ethidium bromide dual staining assay for apoptosis

B16 cells were seeded in 25-cm^2 flasks (Becton Dickinson Labware) at 1.5×10^6 cells/flask with 5 mL medium/flask and incubated for 24 h. Medium was then decanted and cultures were replenished with medium containing geranylgeraniol. Following additional 24-h incubation the monolayer cells were harvested by trypsinization. Cells were re-suspended in 100 μL cold PBS and a dye mixture (4 μL) containing 50 μg/mL acridine orange (Becton, Dickinson and Company, Sparks, MD, USA) and 50 μg/mL ethidium bromide (Sigma-Aldrich) was added to each sample. The cells were then immediately observed under an Axiovert 200 mol/L microscope (Carl Zeiss MicroImaging Inc, Thornwood, NY, USA) equipped with a FluoArc lamp, an AxioCam MRm digital camera system (Carl Zeiss) and AxioVision Rel. 4.3 program (Carl Zeiss). The phase-contrast images of representative fields of each well and the green and red fluorescence emitted by acridine orange and ethidium bromide staining were captured by using bright field phase 2, fluorescein isothiocyanate (FITC) and tetramethylrhodamine isothiocyanate (TRITC) filters, respectively.[23]

ALP activity assay

B16 cells were inoculated in Petri dishes (100 mm × 20 mm; Corning Life Sciences, Wilkes Barre, PA, USA) at 5×10^6 per dish. Following a 24-h incubation, medium was aspirated and replaced with fresh medium containing 0, 30, 60 and 90 μmol/L geranylgeraniol and the incubation continued for additional 48 h. Cells were washed with PBS twice and lysed with 0.5 mL of 0.5% Triton X-100 per dish. Cell lysates were collected and shaken at room temperature for 20 min before being centrifuged at 14,000 rpm for five minutes. In a 96-well plate, 150 μL supernatant was added to 50 μL of working solution from a QuantiChrom™ Alkaline Phosphatase Assay Kit (BioAssay Systems, Hayward, CA, USA) according to the manufacturer's instruction and the absorbance was read at 405 nm with a Tecan Infinite M200 microplate reader (Tecan, Salzburg, Austria). The protein concentration of each sample was determined with a BCA™ Protein Assay Kit (Pierce, Rockford, IL, USA) and ALP activity was normalized based on protein concentrations.

Western blot

Murine B16 melanoma cells cultured in 150-cm^2 flasks (Midwest Scientific, Valley Park, MO, USA) at 5×10^6 per flask were incubated with geranylgeraniol for 12 and 24 h. Following the incubation the growth medium was aspirated and cells were washed with 10 mL ice cold PBS twice and then 150 μL of lysis buffer (50 mmol/L Tris-HCl, pH 8.8, 5 mmol/L EDTA, 1% SDS [sodium dodecyl sulfate]) containing freshly mixed 1% protease inhibitor cocktail (Sigma-Aldrich) was added to the flask. Cells were sonicated (Fisher Scientific) for 45 s and placed in a dry bath incubator (Boekel Scientific, Feasterville, PA, USA) at 90°C for 20 min. The protein concentration of each sample was determined with a BCA™ Protein Assay Kit (Pierce). Samples containing 60 μg proteins were mixed with lamelli buffer (Bio-Rad Laboratories, Hercules, CA, USA) at 1:1 ratio (v/v) and boiled for five minutes before being loaded onto a Mini PROTEAN® 3 (Bio-Rad) electrophoresis unit with a 15% SDS-polyacrylamide gel and run at 150 V for 2–4 h. The proteins were then transferred on to Immobilon-P transfer membrane (Millipore, Bedford, MA, USA) with a Mini Trans-Blot® Cell (Bio-Rad) at 100 mA overnight. The immobilon-P transfer membranes were then incubated in blocking solution (5% non-fat dry milk in PBS) for two hours at room temperature with shaking, rinsed with PBS and then incubated with monoclonal antibodies to cyclin D1 and cyclin-dependent kinase (Cdk) 4 (Cell Signaling Technology, Beverly, MA, USA) at 4°C overnight. After rinsing with PBS containing 0.1% Tween-20 (PBST) for 10 min, the membrane was incubated with a secondary antibody (horseradish peroxidase linked; Cell Signaling Technology; 1:3000 in PBST) for 45 min at room temperature, washed with PBST for 15 min and reacted with a SuperSignal West Pico Chemiluminescence Kit (Pierce) before being photographed at a Chemi Doc XRS imaging system (Bio-Rad). Precision Strep Tactin-HRP (Bio-Rad) protein standards were used to identify the molecular weight of protein bands. A non-specific IgG (Cell Signaling Technology) was used for background control.

Quantitative realtime polymerase chain reaction

Murine B16 melanoma cells cultured in Petri dishes (100 mm × 20 mm, Corning Life Sciences) at 5×10^6 cells per dish were incubated with geranylgeraniol for 24 h. Total cellular RNA was extracted using TRIzol reagent (Invitrogen) according to the manufacturer's protocols. The concentration and purity of the isolated total RNA were determined spectrophotometrically using optical density 260:280 ratio. The integrity of the purified total RNA was verified by detecting a 2:1 ratio for the 28S:18S ribosomal RNA (rRNA) using agarose gel electrophoresis. Samples were run on a 1.5% agarose gel (Tris-acetate [TAE] buffer) at 80 V for 90 min. Gels were soaked in 0.5 μg/mL ethidium bromide for one hour with shaking and then visualized by Chemi Doc XRS imaging system (Bio-Rad). The mRNA expression levels of HMG-CoA reductase gene (GenBank accession number NM_008255) were analyzed by reverse transcription followed by quantitative realtime polymerase chain reaction (qPCR). Total RNA (2 μg) in a 20 μL reaction buffer was reverse transcribed into cDNA using an Oligo $(dT)_{20}$ primer and SuperScript® III First-Strand kit (Invitrogen) following the manufacturer's instructions. cDNA was diluted by 25-fold with 25 μg/mL of acetylated bovine serum albumin

(Invitrogen) and 6 μL of diluted cDNA was amplified in a 25 μL PCR solution containing 250 nmol/L of both forward and reverse primers of the HMG-CoA reductase gene and iQ™ SYBR® Green Supermix (Bio-Rad). The following primer sequences were designed using Vector NTI Advance version 11 software (Invitrogen): forward, GCTTGGGCCAGAGAAGACAGTGCTC; Reverse, ACTCT GCTGACCCCCTGAGGAAGCT. The cDNA was denatured at 95°C for three minutes followed by 40 cycles of PCR (94°C for 30 s, 60°C for 25 s, 72°C for 25 s and 78°C for 9 s) using DNA Engine Opticon® 2 System (Bio-Rad) with the Opticon Monitor program (version 3). The mRNA levels were normalized using ribosomal protein L22 (RPL22) as internal control[24] and quantified by using the δCt method. Fold changes of gene expression were calculated by the 2-$\delta\delta$Ct method.

Statistics

One- or two-way analysis of variance (ANOVA) was performed to assess the differences between groups using Prism® 4.0 software (GraphPad Software Inc, San Diego, CA, USA). Differences in means were analyzed by Dunnett's multiple comparison test unless specified otherwise. Levels of significance were designated as $P < 0.05$.

Results

Figure 1a shows the geranylgeraniol-mediated suppression of the growth of murine B16 melanoma cells and 3T3-L1 fibroblasts. The IC_{50} values, concentrations of geranylgeraniol required to suppress cell growth by 50%, for B16 cells (55 ± 13 μmol/L, $n = 6$) was lower than one-tenth of that for 3T3-L1 cells (>640 μmol/L, $n = 3$), indicating the higher sensitivities of the tumorigenic B16 cells to geranylgeraniol-mediated growth suppression. The photomicrographs shown in Figure 1b reveal the impact of geranylgeraniol on the B16 cells following a 24-h incubation. The untreated cells (I) exhibited the characteristic contact inhibition-disabled growth of B16 cells. Increasing the concentration of geranylgeraniol from 0 to 30 (II) and 60 (III) μmol/L yielded dose-dependent decreases in cell density and marked cell elongation.

Since geranylgeraniol-mediated growth suppression may stem from the down-regulation of HMG-CoA reductase, we then evaluated the impact of supplemental mevalonate, the product of HMG-CoA reductase activity, on geranylgeraniol-induced growth suppression (Figure 2). While geranylgeraniol (30–90 μmol/L) induced concentration-dependent growth suppression, supplemental mevalonate (500 μmol/L) significantly attenuated the effect of geranylgeraniol at all concentrations evaluated.

The effect of geranylgeraniol on HMG-CoA reductase was further demonstrated by realtime qPCR. Following a 24-h incubation with 60 μmol/L geranylgeraniol, B16 cells had a significantly lower level of HMG-CoA mRNA (Mann–Whitney *post hoc* analysis, $n = 4$, $P < 0.05$) with a medium value of 50% of that of control.

HMG-CoA reductase down-regulators have been shown to induce cell cycle arrest at the G1 phase.[5] We then evaluated the impact of geranylgeraniol on the cell cycle distribution of the B16 cells (Figure 3). The percentages of cells at the G1, S and G2 phases prior to incubation with

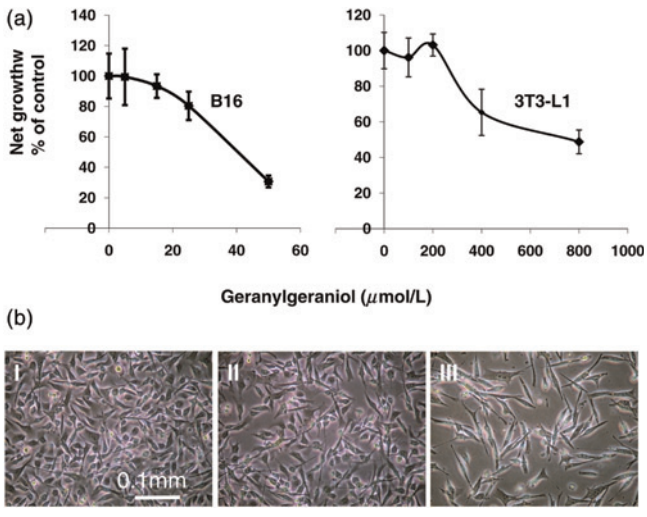

Figure 1 The differential impacts of geranylgeraniol on the growth of murine B16 melanoma cells and murine 3T3-L1 embryo fibroblasts. (a) Representative growth curves showing the concentration-dependent impact of geranylgeraniol on the growth of murine B16 melanoma cells (■) and the impact of geranylgeraniol on 3T3-L1 embryo fibroblasts (◆). Cells were cultured and incubated with geranylgeraniol for 48 h before cell growth was measured by CellTiter 96® Aqueous One Solution. Values are mean ± SD, $n = 4$. (b) The concentration-dependent inhibition of murine B16 melanoma cell growth shown in photomicrographs of B16 cells following a 24-h incubation with 0 (I), 30 (II) and 60 (III) μmol/L geranylgeraniol. The contact inhibition-disabled growth of the B16 cells is shown in the Control culture (I). Concentration-dependent cell elongation and decrease in cell density occur progressively as the concentration of geranylgeraniol is increased (II and III) (A color version of this figure is available in the online journal)

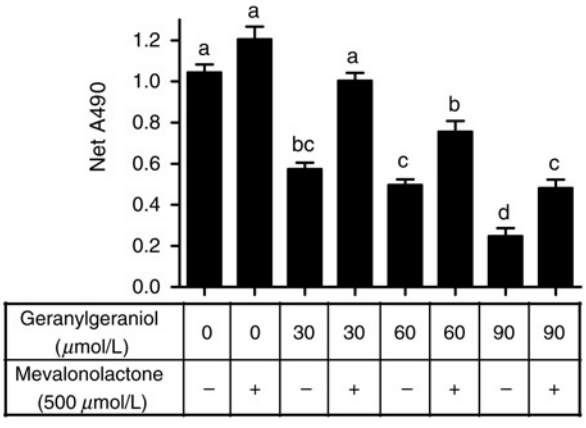

Figure 2 Mevalonolactone (500 μmol/L) attenuates the geranylgeraniol-mediated growth suppression in murine B16 melanoma cells following a 48-h incubation with 0, 30, 60 and 90 μmol/L of geranylgeraniol. Values for net growth measured by net absorbance at 490 nm are mean ± SD, $n = 6$. There were significant effects of geranylgeraniol concentration ($P < 0.001$), mevalonolactone supplementation ($P < 0.001$) and their interaction ($P < 0.05$) based on two-way analysis of variance. All geranylgeraniol groups without mevalonolactone were significantly different from their mevalonolactone-free control (Tukey's, $P < 0.05$). With mevalonolactone supplementation, groups with 60 and 90 μmol/L geranylgeraniol were different from their control (Tukey's, $P < 0.05$). Groups with blends of geranylgeraniol and mevalonolactone were different from their respective mevalonolactone-free groups (Tukey's, $P < 0.05$)

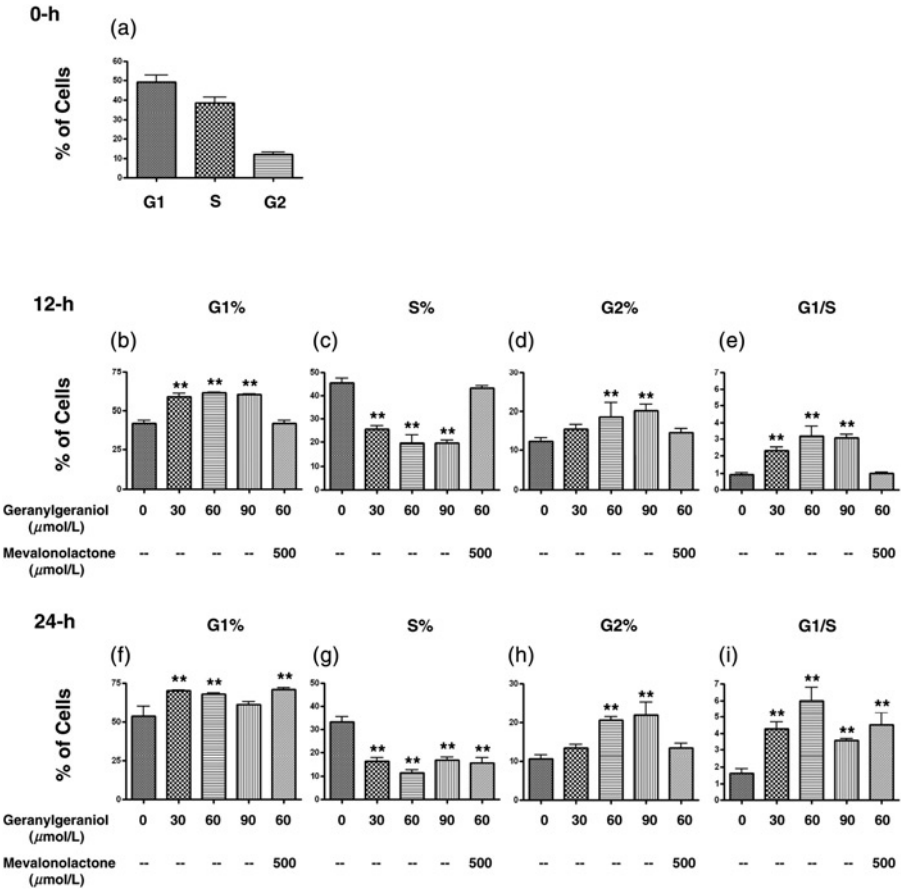

Figure 3 Impact of geranylgeraniol on the cell cycle distribution of murine B16 melanoma cells. The percentages of murine B16 melanoma cells in the G1 (b and f), S (c and g) and G2 (d and h) phases of the cell cycle and the G1/S ratio (e and i) of B16 cells following 0- (a), 12- (b–e) and 24- (f–i) h incubations with 0, 30, 60 and 90 μmol/L geranylgeraniol blended with 0 and 500 μmol/L mevalonolactone are shown. Values are mean $\pm$ SD, $n = 3$. Differences between treated and control (0 μmol/L) groups were analyzed by one-way analysis of variance with Dunnett's post-test ($^{*}P < 0.05$; $^{**}P < 0.01$)

geranylgeraniol were shown in Figure 3a. Following a 12-h incubation with geranylgeraniol, the percentage of cells at the G1 phase increased from $42.2 \pm 1.7\%$ (control) to $59.1 \pm 2.1\%$ (30 μmol/L geranylgeraniol, $P < 0.01$), $61.7 \pm 0.3\%$ (60 μmol/L geranylgeraniol, $P < 0.01$) and $60.3 \pm 0.4\%$ (90 μmol/L geranylgeraniol, $P < 0.01$), respectively. Co-incubation with 500 μmol/L mevalonolactone and 60 μmol/L geranylgeraniol reduced the percentage of cells at the G1 phase ($42.2 \pm 1.9\%$) to the control level (Figure 3b). Conversely, the percentage of cells at the S phase decreased from $45.6 \pm 2.0\%$ (control) to $25.5 \pm 1.6\%$ (30 μmol/L geranylgeraniol, $P < 0.01$), $19.6 \pm 3.3\%$ (60 μmol/L geranylgeraniol, $P < 0.01$) and $19.6 \pm 1.3\%$ (90 μmol/L geranylgeraniol, $P < 0.01$), respectively. Co-incubation with 500 μmol/L mevalonolactone and 60 μmol/L geranylgeraniol increased the percentage of cells at the S phase ($43.3 \pm 0.9\%$, $P > 0.05$) to the control level (Figure 3c). The G1/S ratio, an indicator of cell cycle arrest at the G1 phase, followed the pattern of the G1 phase; that is, the ratio increased from 0.9 ± 0.1 (control) to 2.3 ± 0.2 (30 μmol/L geranylgeraniol, $P < 0.01$), 3.2 ± 0.6 (60 μmol/L geranylgeraniol, $P < 0.01$) and 3.1 ± 0.2 (90 μmol/L geranylgeraniol, $P < 0.01$), respectively. Co-incubation with 500 μmol/L mevalonolactone and 60 μmol/L geranylgeraniol reduced the G1/S ratio (1.0 ± 0.1, $P > 0.05$) to the control level (Figure 3e). The percentage of cells at the G2 phase also increased from $12.4 \pm 0.9\%$ (control) to $15.4 \pm 1.2\%$ (30 μmol/L geranylgeraniol, $P > 0.05$), $18.7 \pm 3.5\%$ (60 μmol/L geranylgeraniol, $P < 0.01$) and $20.1 \pm 1.7\%$ (90 μmol/L geranylgeraniol, $P < 0.01$), respectively. Co-incubation with 500 μmol/L mevalonolactone and 60 μmol/L geranylgeraniol decreased the percentage of cells at the G2 phase ($14.5 \pm 1.0\%$, $P > 0.05$) to the control level (Figure 3d).

Following a 24-h incubation with geranylgeraniol, the percentage of cells at the G1 phase increased from $53.5 \pm 6.5\%$ (control) to $70.1 \pm 0.5\%$ (30 μmol/L geranylgeraniol, $P < 0.01$) and $67.9 \pm 0.7\%$ (60 μmol/L geranylgeraniol, $P < 0.01$), respectively (Figure 3f). Conversely, the percentage of cells at the S phase decreased from $33.3 \pm 2.4\%$ (control) to $16.5 \pm 1.5\%$ (30 μmol/L geranylgeraniol, $P < 0.01$) and $11.4 \pm 1.4\%$ (60 μmol/L geranylgeraniol, $P < 0.01$), respectively (Figure 3g). The G1/S ratio followed the pattern of the G1 phase; that is, the ratio increased from 1.6 ± 0.3 (control) to 4.3 ± 0.4 (30 μmol/L geranylgeraniol, $P < 0.01$) and 6.0 ± 0.8 (60 μmol/L geranylgeraniol, $P < 0.01$), respectively (Figure 3i). Although supplemental mevalonolactone did not significantly change the percentage of cells either in the G1 or in the S phase, co-incubation with 500 μmol/L mevalonolactone and 60 μmol/L

geranylgeraniol reduced the G1/S ratio to 4.5 ± 0.7, a value significantly different ($P < 0.05$) from that for 60 μmol/L geranylgeraniol alone. The percentage of cells at the G2 phase also increased from $10.7 \pm 0.9\%$ (control) to $13.3 \pm 1.0\%$ (30 μmol/L geranylgeraniol, $P > 0.05$) and $20.6 \pm 0.9\%$ (60 μmol/L geranylgeraniol, $P < 0.01$), respectively. Co-incubation with 500 μmol/L mevalonolactone and 60 μmol/L geranylgeraniol decreased the percentage of cells at the G2 phase ($13.3 \pm 1.2\%$, $P > 0.05$) to near the control level (Figure 3h).

The G1 arrest induced by geranylgeraniol was accompanied by a concentration-dependent suppression of the expression of cyclin D1 and Cdk4 (Figure 4), key regulators in the G1/S cell cycle progression.[25] Cells incubated with 90 μmol/L of geranylgeraniol for 12 h had significantly lower expression of cyclin D1 and Cdk4 ($P < 0.01$) than the control. At 24 h, geranylgeraniol and lovastatin induced concentration-dependent decreases in the expression of cyclin D1.

HMG-CoA reductase suppressors also induce tumor cell apoptosis,[5] an effect we examined next in B16 cells using the Guava Nexin™ assay with flow cytometry. The percentage of viable, early apoptotic and late apoptotic and necrotic cells in 12- (Figure 5a2–4) and 24-h (Figure 5a5–7) untreated groups were not different ($P > 0.05$) from the 0-h values prior to incubation with geranylgeraniol (Figure 5a1). Following a 12-h incubation with 90 μmol/L geranylgeraniol the percentage of viable cells (Figure 5a2) decreased significantly ($P < 0.05$) whereas that of early apoptotic cells (Figure 5a3) increased ($P < 0.05$). A greater impact of geranylgeraniol was observed when the incubation was extended to 24 h (Figure 5a5–7). The percentages of viable cells (Figure 5a5) following 24-h incubation with 60 and 90 μmol/L geranylgeraniol decreased significantly ($P < 0.01$) whereas those of late apoptotic and necrotic cells (Figure 5a7) increased ($P < 0.01$). Worth noting is that supplemental mevalonate (500 μmol/L) attenuated the impact of 24-h incubation with 60 μmol/L geranylgeraniol by increasing the percentage of viable cells to the control level. Concurrently, the percentage of late apoptotic and necrotic cells also dropped to the control level when 60 μmol/L geranylgeraniol was blended with mevalonate (Figure 5a7). The high level of late apoptotic cells following the 24-h incubation with 90 μmol/L geranylgeraniol may have contributed to the lack of increase in the percentage of cells in the G1 phase (Figure 3f).

Photomicrographs of B16 cells (Figure 5b) obtained by acridine orange and ethidium bromide dual staining also confirmed geranylgeraniol-induced apoptosis. Viable cells have acridine orange staining with normal cell morphology. Acridine orange and ethidium bromide stained cells with condensed nucleus are in early and late apoptosis stages, respectively.[23,26] The number and percentage of ethidium bromide stained B16 cells following 24-h incubation with 75 μmol/L, or a mid-range value between 60 and 90 μmol/L, of geranylgeraniol (Figure 5b7) were higher than the control (Figure 5b3). Geranylgeraniol-treated cells showed nuclear condensation and membrane blebbing (Figures 5b6 and 7), morphological characteristics of apoptosis.

We then examined the impact of geranylgeraniol on ALP activity, a biomarker upregulated during differentiation.[27] Geranylgeraniol induced ALP activity in B16 cells (Figure 6). The ALP activities for B16 cells incubated with 0, 30, 60 and 90 μmol/L geranylgeraniol for 48 h were 0.29 ± 0.02 (IU/L), 0.57 ± 0.00 ($P < 0.01$), 0.55 ± 0.01 ($P < 0.05$) and 0.77 ± 0.14 ($P < 0.001$), with all geranylgeraniol-treated groups significantly different from the control.

Previously studies have shown that mevalonate suppressors have potentially synergistic impact on cell growth.[28,29] Next, we evaluated the potential synergy attained with blends of geranylgeraniol and *d*-δ-tocotrienol, a vitamin E isomer with HMG-CoA reductase-[30,31] and tumor-[32] suppressive activities, in suppressing the growth of B16 cells. Geranylgeraniol at 15 μmol/L and *d*-δ-tocotrienol at 10 μmol/L suppressed the growth of B16 cells by 11% and 24%, respectively; a blend of the agents suppressed cell growth by 39% (Table 1), approximating the sum of individual impacts and indicating an additive effect. The cumulative effect was also shown with the blend containing 15 μmol/L geranylgeraniol and 20 μmol/L *d*-δ-tocotrienol.

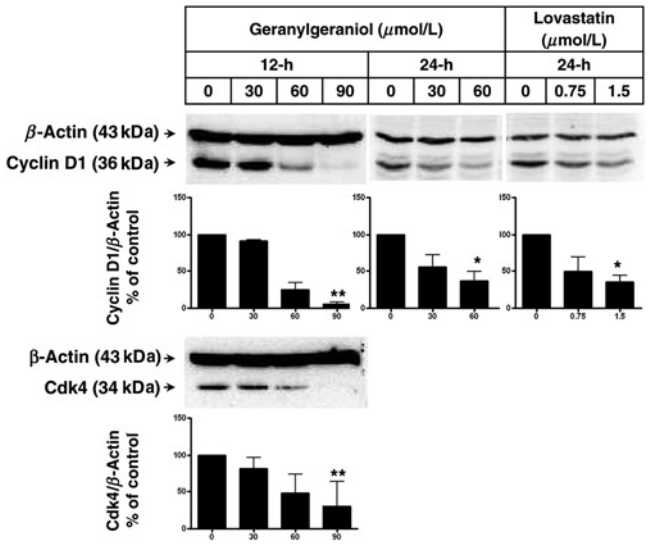

Figure 4 Impact of geranylgeraniol and lovastatin on the expression of cyclin-dependent kinase (Cdk) 4 and cyclin D1 in murine B16 melanoma cells following 12- and 24-h incubations shown in representative blots. Cell lysates were subjected to Western blot procedures and blots were detected by chemiluminescence and quantitated. The values for the ratios of Cdk4/β-actin and cyclin D1/β-actin shown in the bar graphs are median $\pm$ range, $n \geq 3$. Values with * and ** are significantly different from that of control with $P < 0.05$ and $P < 0.01$, respectively, based on Kruskal–Wallis test followed by Dunnett's multiple comparison test

Discussion

Diverse cell lines have a wide range of sensitivity to geranylgeraniol-mediated growth suppression, with IC_{50} values ranging from 10 μmol/L for human HuH-7 hepatoma cells[18] to 400 μmol/L for human H460 lung adenocarcinoma cells;[16] those for other tumor cells originated from pancreas,[14,20] stomach, colon, liver, blood and ovary[14] fall somewhere in between. The IC_{50} value for geranylgeraniol

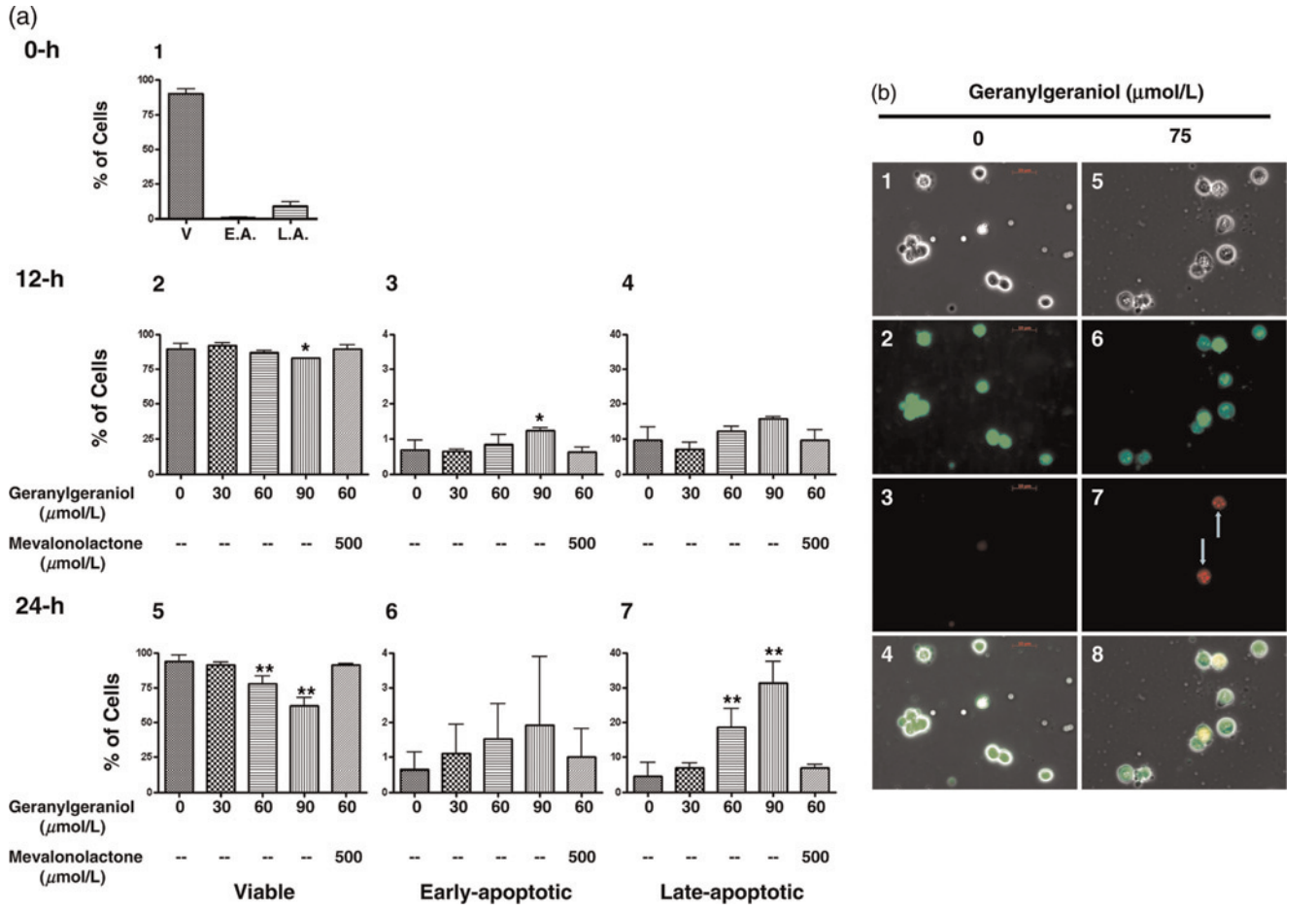

Figure 5 Impact of geranylgeraniol on the initiation of apoptosis in murine B16 melanoma cells. (a) The percentages of viable (V), early-apoptotic (EA) and late-apoptotic and necrotic (LA) B16 cells following 0- (1), 12- (2–4) and 24- (5–7) h incubations with geranylgeraniol as measured by the Guava Nexin™ assay. The percentages of V, EA and LA cells prior to geranylgeraniol incubation are shown in (1). Following a 12-h incubation with 90 μmol/L geranylgeraniol, the percentage of viable cells (2) decreased; concomitantly, the percentage of early apoptotic cells (3) increased. A 24-h incubation with 60 and 90 μmol/L geranylgeraniol led to decreased percentage of viable cells (5) and increased percentage of late apoptotic cells (7). Supplemental mevalonolactone significantly attenuated the impact of 24-h geranylgeraniol incubation on the percentages of viable (5) and late apoptotic and necrotic (7) cells. Values are mean ± SD, $n = 3$. Differences between treated and control (0 μmol/L) groups were analyzed by one-way ANOVA with Dunnett's post-test ($^{*}P < 0.05$; $^{**}P < 0.01$). (b) Photomicrographs of murine B16 melanoma cells showing the geranylgeraniol-initiated apoptosis detected by acridine orange and ethidium bromide dual staining. B16 cells were incubated with 0 (1–4) and 75 (5–8) μmol/L geranylgeraniol for 24 h. Photomicrographs of the same fields were taken under phase-contrast microscope (1 and 5) and fluorescence microscope with a FITC (2 and 6) or TRITC (3 and 7) filter and then merged (4 and 8). Arrows mark the red fluorescence emission from ethidium bromide staining shown in late apoptotic and necrotic cells induced by geranylgeraniol.

in B16 cells evaluated herein lies in the mid-range of the reported IC_{50} values. The underlying mechanisms for such a wide range of sensitivities remain unknown, though they may be related to culture conditions including cell density and length of treatment and potentially the differential extent of dysregulation of the mevalonate pathway in various cell lines. The cell growth assay employed in this study does not differentiate cytostatic and cytotoxic effects that could both lead to decreased cell numbers. The morphological changes induced by geranylgeraniol are reminiscent of those effected by other mevalonate suppressors including lovastatin and tocotrienols.[28]

The geranylgeraniol-induced concentration-dependent impact on cell cycle distribution of B16 cells is consistent with the G1 arrest mediated by geranylgeraniol in A549 cells.[17] Lovastatin[33,34] and other isoprenoid mevalonate suppressors including the monoterpenes perillyl alcohol and geraniol,[35] sesquiterpenes *trans, trans*-farnesol[35] and β-ionone,[5,36] and tocotrienols[5] have been shown to induce G1 arrest in tumor cells. Mevalonate attenuated the lovastatin-mediated G1 arrest in human T24 bladder carcinoma cells[37] and MCF-7 breast cancer cells.[38] The geranylgeraniol-mediated down-regulation of cyclin D1 and Cdk4, two regulators of the G1 to S transition, is consistent with the upregulation of p21 and p27, two suppressors of cyclin D1 and Cdk4,[39] and down-regulation of cyclin D1 and Cdk4 induced by other mevalonate suppressors including lovastatin,[40] perillyl alcohol,[35] geraniol,[35,41] farnesol,[35] β-ionone[41] and lycopene.[42] Mevalonate attenuated the lovastatin-mediated upregulation of p21 and p27 in MDA-MB-157 tumor cells.[40]

Geranylgeraniol-induced B16 cell apoptosis is consistent with previous reports in A549 lung adenocarcinoma cells,[11,17] HL-60,[12,13,43] K562,[12,13] ML1, M1, P388[43] and U937[15,43] leukemia cells, COLO320 DM colon adenocarcinoma cells,[13] HuH-7 hepatoma cells,[18] and TYK-nu ovarian cancer cells.[19] Geranylgeraniol also activates caspase-3[15,18,44] and PARP cleavage.[44] The concentration of geranylgeraniol

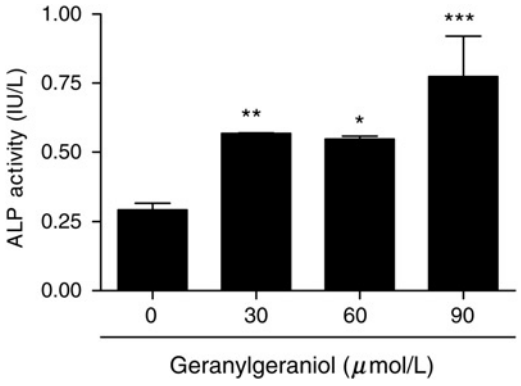

Figure 6 Impact of geranylgeraniol on alkaline phosphatase (ALP) activity in murine B16 melanoma cells. Following a 48-h incubation with 0, 30, 60 and 90 μmol/L geranylgeraniol, B16 cells were lysed and ALP activity in the supernatant was analyzed using a QuantiChrom™ Alkaline Phosphatase Assay Kit as described in Materials and Methods. Values are mean $\pm$ SD, $n = 3$. Values with *, ** and *** are significantly different from that of control with $P < 0.05$, $P < 0.01$ and $P < 0.001$, respectively, as determined by one-way analysis of variance with Tukey's multiple comparison test

required to induce apoptosis in these studies[12,13,15,17] falls in the 30–90 μmol/L range employed in the present study for the induction of apoptosis in B16 cells (Figure 5).

Geranylgeraniol-induced ALP activity, an indicator of B16 cell differentiation, is reminiscent of the geranylgeranylacetone-induced differentiation of human U937, ML1 and HL-60 myeloid leukemia cells.[45] Consequently, menaquinone 4[46,47] with a geranylgeraniol moiety, rather than phylloquinone[46] with a phytol side chain, is able to induce differentiation.

Parallel to the impact of geranylgeraniol, mevalonate suppressors[48] including the monoterpenes,[49] sodium phenylacetate, sodium phenylbutyrate,[50] lovastatin[51,52] and genistein[53] induce tumor cell differentiation.

Mevalonate suppressors have been shown to induce cell cycle arrest, apoptosis and differentiation, consequent to the impaired post-translational modification of Ras,[26] insulin-like growth factor 1 receptor[48] and nuclear lamins.[5] These events may have collectively contributed to the geranylgeraniol-induced growth suppression. Supplemental mevalonolactone attenuated growth suppression, cell cycle arrest and apoptosis, further supporting our hypothesis that the suppression of HMG-CoA reductase activity, at least in part, mediates the impact of geranylgeraniol in B16 cells. Previous studies have shown that geranylgeraniol suppresses reductase activity in fibroblasts,[9,10] human A549 lung adenocarcinoma cells[11] and human MCF-7 breast adenocarcinoma cells;[54] mevalonate attenuated the geranylgeraniol impact in MCF-7 cells.[54] The IC_{50} value (55 μmol/L) of geranylgeraniol in suppressing the growth of B16 cells equals to that required to suppress HMG-CoA reductase by 50% in A549 cells[11] and MCF-7 cells[54] and in the current study, that required to suppress the mRNA level for HMG-CoA reductase by 50%. Consequent to HMG-CoA reductase down-regulation, gavage feeding of geranylgeraniol reduced plasma cholesterol level in Wistar rats and, more prominently, reduced tumor incidence and the size of preneoplastic lesions in chemically initiated hepatocarcinogenesis.[55]

Previous studies have used mevalonate at concentrations ranging from 500 μmol/L[54] to 4 mmol/L[40] to show its ability to reverse the effects of mevalonate suppressors including geranylgeraniol and lovastatin. Though at the lower end of that range, the 500 μmol/L mevalonolactone used herein far exceeds physiologically attainable levels. It is conceivable that secondary effects of the pharmaceutical level of mevalonate beyond the repletion of cellular mevalonate pool may have interfered with the impact of geranylgeraniol. *In vivo* studies may provide more direct evidence linking the reductase- and tumor-suppressive activities of geranylgeraniol. Nevertheless, the present study may have identified mevalonate depletion as a unifying mechanism for geranylgeraniol-mediated tumor suppression.

The concentration of geranylgeraniol, 100 μmol/L, employed to suppress reductase in fibroblasts[9] is twice as high as that in the A549 cells,[11] MCF-7 cells[54] and the B16 cells herein. In the present study, murine 3T3-L1 cells were more than 10-fold resistant than B16 cells to geranylgeraniol-mediated growth suppression, suggesting a tumor-targeting action of geranylgeraniol. Geranylgeraniol may be added to the growing list of isoprenoids with specific impact on the uniquely dysregulated HMG-CoA reductase in tumors.[48] It remains unknown whether the reductase is dysregulated in B16 melanoma cells.

Blends of mevalonate suppressors synergistically suppress tumor growth.[28,29,48] The additive effect of geranylgeraniol and *d*-δ-tocotrienol in suppressing B16 cell growth could reflect their dual impact on HMG-CoA reductase. *In vivo* and further mechanistic studies may reveal whether geranylgeraniol and a broad class of mevalonate-derived secondary products, the pure and mixed isoprenoids with reductase-suppressive activities, have potential in cancer chemoprevention and/or therapy when applied individually and in blends.

Table 1 Cumulative impact of geranylgeraniol and *d*-δ-tocotrienol on the proliferation of murine B16 melanoma cells

	Growth	Suppression % of control
Control	$100 \pm 6^{a*}$	
Geranylgeraniol (15 μmol/L)	89 ± 4^{ab}	11
d-δ-Tocotrienol (10 μmol/L)	76 ± 13^{bc}	24
d-δ-Tocotrienol (20 μmol/L)	44 ± 10^{de}	56
Geranylgeraniol (15 μmol/L) + *d*-δ-Tocotrienol (10 μmol/L)	61 ± 4^{cd}	39 (35)†
Geranylgeraniol (15 μmol/L) + *d*-δ-Tocotrienol (20 μmol/L)	29 ± 4^{e}	71 (67)

*Values are mean $\pm$ SD, $n = 3$. Means that are not denoted with a common letter are different ($P < 0.05$) based on one-way analysis of variance with Tukey's multiple comparison test

†Numbers in the parentheses indicate expected percentage of growth suppression based on the sum of individual suppressions

Author contributions: All authors participated in the design, interpretation of the studies and analysis of the data and review of the manuscript. RK, NVF, ME, DD, NM and DLH conducted the experiments. HM, CK and DLH contributed to the conceptualization of the studies. HM wrote the manuscript.

ACKNOWLEDGEMENTS

We thank Dr Heather Conrad-Webb of the Biology Department for her assistance with the BD FACSCalibur. This study was supported by the Texas Department of Agriculture and Texas Woman's University Research Enhancement Program, Summer Stipend Award and Human Nutrition Research Fund.

REFERENCES

1 Hutchison CJ, Bridger JM, Cox LS, Kill IR. Weaving a pattern from disparate threads: lamin function in nuclear assembly and DNA replication. *J Cell Sci* 1994;**107**:3259–69
2 Crowell PL, Chang RR, Ren ZB, Elson CE, Gould MN. Selective inhibition of isoprenylation of 21–26-kDa proteins by the anticarcinogen d-limonene and its metabolites. *J Biol Chem* 1991;**266**:17679–85
3 Goldstein JL, Brown MS. Regulation of the mevalonate pathway. *Nature* 1990;**343**:425–30
4 Elson CE, Peffley DM, Hentosh P, Mo H. Isoprenoid-mediated inhibition of mevalonate synthesis: potential application to cancer. *Proc Soc Exp Biol Med* 1999;**221**:294–311
5 Mo H, Elson CE. Apoptosis and cell-cycle arrest in human and murine tumor cells are initiated by isoprenoids. *J Nutr* 1999;**129**:804–13
6 Fedeli E, Capella P, Cirimele M, Jacini G. Isolation of geranyl geraniol from the unsaponifiable fraction of linseed oil. *J Lipid Res* 1966;**7**:437–41
7 Myers CE, Trepel J, Sausville E, Samid D, Miller A, Curt G. Monoterpenes, sesquiterpenes and diterpenes as cancer therapy. United States Patent 5,602,184, 1997
8 Mors WB, dos Santos Filho MF, Monteiro HJ, Gilbert B, Pellegrino J. Chemoprophylactic agent in schistosomiasis: 14,15-epoxygeranylgeraniol. *Science* 1967;**157**:950–1
9 Sever N, Song BL, Yabe D, Goldstein JL, Brown MS, DeBose-Boyd RA. Insig-dependent ubiquitination and degradation of mammalian 3-hydroxy-3-methylglutaryl-CoA reductase stimulated by sterols and geranylgeraniol. *J Biol Chem* 2003;**278**:52479–90
10 Houten SM, Schneiders MS, Wanders RJ, Waterham HR. Regulation of isoprenoid/cholesterol biosynthesis in cells from mevalonate kinase-deficient patients. *J Biol Chem* 2003;**278**:5736–43
11 Miquel K, Pradines A, Favre G. Farnesol and geranylgeraniol induce actin cytoskeleton disorganization and apoptosis in A549 lung adenocarcinoma cells. *Biochem Biophys Res Commun* 1996;**225**:869–76
12 Ohizumi H, Masuda Y, Yoda M, Hashimoto S, Aiuchi T, Nakajo S, Sakai I, Ohsawa S, Nakaya K. Induction of apoptosis in various tumor cell lines by geranylgeraniol. *Anticancer Res* 1997;**17**:1051–7
13 Ohizumi H, Masuda Y, Nakajo S, Sakai I, Ohsawa S, Nakaya K. Geranylgeraniol is a potent inducer of apoptosis in tumor cells. *J Biochem (Tokyo)* 1995;**117**:11–3
14 Shibayama-Imazu T, Sakairi S, Watanabe A, Aiuchi T, Nakajo S, Nakaya K. Vitamin K(2) selectively induced apoptosis in ovarian TYK-nu and pancreatic MIA PaCa-2 cells out of eight solid tumor cell lines through a mechanism different from geranylgeraniol. *J Cancer Res Clin Oncol* 2003;**129**:1–11
15 Masuda Y, Nakaya M, Nakajo S, Nakaya K. Geranylgeraniol potently induces caspase-3-like activity during apoptosis in human leukemia U937 cells. *Biochem Biophys Res Commun* 1997;**234**:641–5
16 Joo JH, Liao G, Collins JB, Grissom SF, Jetten AM. Farnesol-induced apoptosis in human lung carcinoma cells is coupled to the endoplasmic reticulum stress response. *Cancer Res* 2007;**67**:7929–36
17 Miquel K, Pradines A, Terce F, Selmi S, Favre G. Competitive inhibition of choline phosphotransferase by geranylgeraniol and farnesol inhibits phosphatidylcholine synthesis and induces apoptosis in human lung adenocarcinoma A549 cells. *J Biol Chem* 1998;**273**:26179–86
18 Takeda Y, Nakao K, Nakata K, Kawakami A, Ida H, Ichikawa T, Shigeno M, Kajiya Y, Hamasaki K, Kato Y, Eguchi K. Geranylgeraniol, an intermediate product in mevalonate pathway, induces apoptotic cell death in human hepatoma cells: death receptor-independent activation of caspase-8 with down-regulation of Bcl-xL expression. *Jpn J Cancer Res* 2001;**92**:918–25
19 Shibayama-Imazu T, Sonoda I, Sakairi S, Aiuchi T, Ann WW, Nakajo S, Itabe H, Nakaya K. Production of superoxide and dissipation of mitochondrial transmembrane potential by vitamin K2 trigger apoptosis in human ovarian cancer TYK-nu cells. *Apoptosis* 2006;**11**:1535–43
20 Burke YD, Stark MJ, Roach SL, Sen SE, Crowell PL. Inhibition of pancreatic cancer growth by the dietary isoprenoids farnesol and geraniol. *Lipids* 1997;**32**:151–6
21 McAnally JA, Jung M, Mo H. Farnesyl-*O*-acetylhydroquinone and geranyl-*O*-acetylhydroquinone suppress the proliferation of murine B16 melanoma cells, human prostate and colon adenocarcinoma cells, human lung carcinoma cells, and human leukemia cells. *Cancer Lett* 2003;**202**:181–92
22 Fernandes N, Jung M, Daoud A, Mo H. Biphenylalkylacetylhydroquinone ethers suppress the proliferation of murine B16 melanoma cells. *Anticancer Res* 2008;**28**:1005–12
23 Hussein D, Mo H. *d*-δ-Tocotrienol-mediated suppression of the proliferation of human PANC-1, MIA PaCa2 and BxPC-3 pancreatic carcinoma cells. *Pancreas* 2009;**38**:e124–36
24 de Jonge HJ, Fehrmann RS, de Bont ES, Hofstra RM, Gerbens F, Kamps WA, de Vries EG, van der Zee AG, te Meerman GJ, ter Elst A. Evidence based selection of housekeeping genes. *PLoS One* 2007;**2**:e898
25 Massague J. G1 cell-cycle control and cancer. *Nature* 2004;**432**:298–306
26 Fernandes NV, Guntipalli PK, Mo H. *d*-δ-Tocotrienol-mediated cell cycle arrest and apoptosis in human melanoma cells. *Anticancer Res* 2010;**30**:4937–44
27 Yamada T, Ohwada S, Saitoh F, Adachi M, Morishita Y, Hozumi M. Induction of Ley antigen by 5-aza-2′-deoxycytidine in association with differentiation and apoptosis in human pancreatic cancer cells. *Anticancer Res* 1996;**16**:735–40
28 McAnally JA, Gupta J, Sodhani S, Bravo L, Mo H. Tocotrienols potentiate lovastatin-mediated growth suppression in vitro and in vivo. *Exp Biol Med (Maywood)* 2007;**232**:523–31
29 Tatman D, Mo H. Volatile isoprenoid constituents of fruits, vegetables and herbs cumulatively suppress the proliferation of murine B16 melanoma and human HL-60 leukemia cells. *Cancer Lett* 2002;**175**:129–39
30 Parker RA, Pearce BC, Clark RW, Gordon DA, Wright JJ. Tocotrienols regulate cholesterol production in mammalian cells by post-transcriptional suppression of 3-hydroxy-3-methylglutaryl-coenzyme A reductase. *J Biol Chem* 1993;**268**:11230–8
31 Song BL, DeBose-Boyd RA. Insig-dependent ubiquitination and degradation of 3-hydroxy-3-methylglutaryl coenzyme a reductase stimulated by δ- and γ-tocotrienols. *J Biol Chem* 2006;**281**:25054–61
32 Mo H, Elson CE. Role of the mevalonate pathway in tocotrienol-mediated tumor suppression. In: Watson RR, Preedy VR, eds. *Tocotrienols: Vitamin E Beyond Tocopherols*. Boca Raton: CRC Press, 2008: 185–207
33 Rao S, Lowe M, Herliczek TW, Keyomarsi K. Lovastatin mediated G1 arrest in normal and tumor breast cells is through inhibition of CDK2 activity and redistribution of p21 and p27, independent of p53. *Oncogene* 1998;**17**:2393–402
34 Park C, Lee I, Kang WK. Lovastatin-induced E2F-1 modulation and its effect on prostate cancer cell death. *Carcinogenesis* 2001;**22**:1727–31
35 Wiseman DA, Werner SR, Crowell PL. Cell cycle arrest by the isoprenoids perillyl alcohol, geraniol, and farnesol is mediated by p21(Cip1) and p27(Kip1) in human pancreatic adenocarcinoma cells. *J Pharmacol Exp Ther* 2007;**320**:1163–70
36 He L, Mo H, Hadisusilo S, Qureshi AA, Elson CE. Isoprenoids suppress the growth of murine B16 melanomas in vitro and in vivo. *J Nutr* 1997;**127**:668–74
37 Jakobisiak M, Bruno S, Skierski JS, Darzynkiewicz Z. Cell cycle-specific effects of lovastatin. *Proc Natl Acad Sci USA* 1991;**88**:3628–32
38 Keyomarsi K, Sandoval L, Band V, Pardee AB. Synchronization of tumor and normal cells from G1 to multiple cell cycles by lovastatin. *Cancer Res* 1991;**51**:3602–9
39 Sherr CJ. Mammalian G1 cyclins. *Cell* 1993;**73**:1059–65
40 Gray-Bablin J, Rao S, Keyomarsi K. Lovastatin induction of cyclin-dependent kinase inhibitors in human breast cells occurs in a cell cycle-independent fashion. *Cancer Res* 1997;**57**:604–9
41 Duncan RE, Lau D, El-Sohemy A, Archer MC. Geraniol and β-ionone inhibit proliferation, cell cycle progression, and cyclin-dependent

kinase 2 activity in MCF-7 breast cancer cells independent of effects on HMG-CoA reductase activity. *Biochem Pharmacol* 2004;**68**:1739–47

42 Palozza P, Colangelo M, Simone R, Catalano A, Boninsegna A, Lanza P, Monego G, Ranelletti FO. Lycopene induces cell growth inhibition by altering mevalonate pathway and Ras signaling in cancer cell lines. *Carcinogenesis* 2010;**31**:1813–21

43 Masuda Y, Yoda M, Ohizumi H, Aiuchi T, Watabe M, Nakajo S, Nakaya K. Activation of protein kinase C prevents induction of apoptosis by geranylgeraniol in human leukemia HL60 cells. *Int J Cancer* 1997;**71**:691–7

44 Au-Yeung KK, Liu PL, Chan C, Wu WY, Lee SS, Ko JK. Herbal isoprenols induce apoptosis in human colon cancer cells through transcriptional activation of PPARgamma. *Cancer Invest* 2008;**26**:708–17

45 Sakai I, Tanaka T, Osawa S, Hashimoto S, Nakaya K. Geranylgeranylacetone used as an antiulcer agent is a potent inducer of differentiation of various human myeloid leukemia cell lines. *Biochem Biophys Res Commun* 1993;**191**:873–9

46 Sakai I, Hashimoto S, Yoda M, Hida T, Ohsawa S, Nakajo S, Nakaya K. Novel role of vitamin K2: a potent inducer of differentiation of various human myeloid leukemia cell lines. *Biochem Biophys Res Commun* 1994;**205**:1305–10

47 Takami A, Nakao S, Ontachi Y, Yamauchi H, Matsuda T. Successful therapy of myelodysplastic syndrome with menatetrenone, a vitamin K2 analog. *Int J Hematol* 1999;**69**:24–6

48 Mo H, Elson CE. Studies of the isoprenoid-mediated inhibition of mevalonate synthesis applied to cancer chemotherapy and chemoprevention. *Exp Biol Med (Maywood)* 2004;**229**:567–85

49 Shi W, Gould MN. Induction of differentiation in neuro-2A cells by the monoterpene perillyl alcohol. *Cancer Lett* 1995;**95**:1–6

50 Melichar B, Ferrandina G, Verschraegen CF, Loercher A, Abbruzzese JL, Freedman RS. Growth inhibitory effects of aromatic fatty acids on ovarian tumor cell lines. *Clin Cancer Res* 1998;**4**:3069–76

51 Maltese WA. Induction of differentiation in murine neuroblastoma cells by mevinolin, a competitive inhibitor of 3-hydroxy-3-methylglutaryl coenzyme A reductase. *Biochem Biophys Res Commun* 1984;**120**:454–60

52 Dimitroulakos J, Thai S, Wasfy GH, Hedley DW, Minden MD, Penn LZ. Lovastatin induces a pronounced differentiation response in acute myeloid leukemias. *Leuk Lymphoma* 2000;**40**:167–78

53 Record IR, Broadbent JL, King RA, Dreosti IE, Head RJ, Tonkin AL. Genistein inhibits growth of B16 melanoma cells *in vivo* and *in vitro* and promotes differentiation in vitro. *Int J Cancer* 1997;**72**:860–4

54 Raikkonen J, Monkkonen H, Auriola S, Monkkonen J. Mevalonate pathway intermediates downregulate zoledronic acid-induced isopentenyl pyrophosphate and ATP analog formation in human breast cancer cells. *Biochem Pharmacol* 2010;**79**:777–83

55 de Moura Espindola R, Mazzantini RP, Ong TP, de Conti A, Heidor R, Moreno FS. Geranylgeraniol and β-ionone inhibit hepatic preneoplastic lesions, cell proliferation, total plasma cholesterol and DNA damage during the initial phases of hepatocarcinogenesis, but only the former inhibits NF-κB activation. *Carcinogenesis* 2005;**26**:1091–9

(Received December 16, 2010, Accepted February 22, 2011)